Editors' Suggestion

Exploration-Exploitation Paradigm for Networked Biological Systems

Vito Dichio and Fabrizio De Vico Fallani*
Sorbonne Universite, Paris Brain Institute-ICM, CNRS, Inria, Inserm, AP-HP, Hopital de la Pitie Salpêtriere, F-75013, Paris, France

(Received 30 June 2023; accepted 24 January 2024; published 1 March 2024)

The stochastic exploration of the configuration space and the exploitation of functional states underlie many biological processes. The evolutionary dynamics stands out as a remarkable example. Here, we introduce a novel formalism that mimics evolution and encodes a general exploration-exploitation dynamics for biological networks. We apply it to the brain wiring problem, focusing on the maturation of that of the nematode *Caenorhabditis elegans*. We demonstrate that a parsimonious maxent description of the adult brain combined with our framework is able to track down the entire developmental trajectory.

DOI: 10.1103/PhysRevLett.132.098402

Introduction.—Modeling and analyzing the dynamics of biological systems is notoriously challenging. Critically, they are often stochastic in nature, as they involve and possibly exploit some degree of randomness. At the same time, biological dynamics are also shaped by functional constraints that determine which outcomes are viable. The constraints emerge from the need for biological systems to perform specific tasks and act on the system as a whole, not on specific components. Stochastic events that violate these constraints are unlikely to persist, while those that align with them are more likely to become integrated. If the details of such exploration-exploitation (EE) dynamics are context dependent, general principles can still be formulated [1]. This entails addressing several challenging questions. For instance, how do biological systems explore the space of possible configurations? How do they identify the optimal states that satisfy specific functional demands?

A possible solution is offered by nature itself. In evolutionary dynamics, a population primarily evolves under the combined action of mutations and recombinations (exploration) and natural selection (exploitation). The latter is based on the notion of fitness: Those individuals that are more apt to the environment will have a higher reproductive success (high fitness) and survive to the next generations, while the others will go extinct [2] (see Supplemental Material, Sec. I [3]). We argue that evolutionary dynamics is a particular instance of the aforementioned EE dynamics and build upon it to construct a general EE formalism for networked biological systems.

We use it to tackle the brain wiring problem and model the developmental dynamics of the *Caenorhabditis elegans* connectome, recently obtained by serial-section electron microscopy [4,5,33].

Theoretical framework.—Let us begin by clarifying the terminology. (a) Exploration refers to the act of stochastically searching the configuration space. (b) Exploitation refers to the harnessing the discovered configurations to optimize the system function. The resulting optimization problem is defined once we specify (b)(i) how the optimal states are encoded and (b)(ii) how the system approaches them.

Formally, let us consider a biological system represented as a simple graph (or network) $G \in \mathcal{G}$ over N nodes, unweighted, undirected, with no self-loops. It can be identified with a finite, binary, symmetric and with zero-diagonal adjacency matrix $G = \{a_{ij}\}$, where $a_{ij} \in \{0, 1\}$ indicates the absence or presence of an edge within the pair of nodes, or dyad, (ij). There are $L = N(N-1)/2$ dyads and, hence, L possible edges. Let $P(G, t)$ be the probability of the graph G at time t.

(a) *Exploration.*—Each dyad mutates its state in the time interval Δt with rate $\mu \geq 0$. A simple exploration scheme is to randomly create or dissolve edges; e.g., an edge is added if none existed or removed if present. The effect on the graph distribution is

$$P(G, t + \Delta t) = P(G, t) + \Delta t \mu \sum_{i<j} \left[P(M_{ij} G, t) - P(G, t) \right], \tag{1}$$

where M_{ij} is the operator that mutates the dyad a_{ij} of the graph G. The exploration rate μ is here constant and uniform across dyads.

(b) *Exploitation.*—A functional metric $F(G) : \mathcal{G} \to \mathbb{R}$ serves the purpose of representing the concept of biological function, with optimal states defined as maxima of F (b)(i). In the time interval Δt, we formally define exploitation as follows:

$$P(G, t + \Delta t) = \frac{e^{\Delta t \varphi F(G)}}{\langle e^{\Delta t \varphi F} \rangle_t} P(G, t), \tag{2}$$

where $\langle \cdot \rangle_t$ stands for the ensemble average at time t, i.e., $\langle e^{\Delta t \varphi F} \rangle_t = \sum_G e^{\Delta t \varphi F(G)} P(G, t)$, and $\varphi \geq 0$, the

exploitation rate, is an overall scaling. Therefore, the way in which the dynamics approach the most functional (highest F) configurations is by exponentially increasing the probability of those graphs that have higher F values than the ensemble average at time t (b)(ii).

We will refer to the ratio $\rho = \varphi/\mu$ as the functional pressure: $\rho \sim 0$ implies a dynamic dominated by randomness, similar to a random walk in the graph space $\mathcal{G}$, while $\rho \to \infty$ corresponds to the limit of perfect exploitation, where only the most functional graph configurations have non-negligible probabilities.

In Supplemental Material, Sec. II [3], we introduce four simple models, namely, the cases of no exploitation, edge penalty, edge covariate, and distancelike F metric. We show that these cases can be treated analytically and offer a formal understanding of the intuitions (i) that the optimal states implied by a F metric are not strictly attainable as long as $\mu \neq 0$ and (ii) that the functional pressure ρ controls not only the rate of approach to the maxima of F, but also the final stationary state.

The above framework closely mimics a Darwinian evolution driven by mutations and fitness-based natural selection, in the infinite population limit [6,32]. Equations (1) and (2) can be regarded as an algorithm, inspired by evolution, that (a) uses random choices to (b) direct an exploitative search for solving an optimization problem. In this sense, it is similar to a genetic algorithm [7]; see Supplemental Material, Sec. I [3]. We further explore the parallel with the evolutionary dynamics to design simulations based on Eqs. (1) and (2), concisely described in Supplemental Material, Sec. III [3].

F is shaped by the environment and has the role of mapping the functional requirements of the biological system onto the configuration space. As a consequence, the particular form of F depends on the specific context and system. In general, no demands are made on the properties of F, which could be regarded as a black box which returns a real number for each possible input (graph). In this work, however, we will study a white-box F metric which admits a mathematical formulation. In particular, we will describe the state of a graph G by a set of *sufficient statistics* $\boldsymbol{x}(G) \in \mathbb{R}^r$, and in this latter space the $F\colon \mathbb{R}^r \to \mathbb{R}$ will be formally defined.

C. elegans brain maturation.—In the following, we will consider the so-called brain wiring problem [33], i.e., how the structural complexity of a natural brain arises during the development of an organism. Answering the brain wiring problem is an open challenge in neuroscience and entails tackling at least two kind of questions: (i) what drives the brain maturation (*structural principles*) and (ii) which is the driving algorithm (*dynamical principles*). Here, we will formulate them in terms of an F metric and EE dynamics, respectively. In particular, the latter is consistent with three essential and general features of the brain wiring dynamics, which are (a) *functionally robust*—the adult brains are capable of supporting the functions that sustain the life of an organism; (b) *not hardwired*—genetically encoded developmental algorithms give rise to similar yet nonidentical structures, resulting in high interindividual variability [33]; and (c) *self-referential*—the updating rules evolve in time, as a function of the state and, therefore, of the history of the system [34].

To tackle the brain wiring problem, a natural choice is to consider that of the nematode *C. elegans* [8] (see Supplemental Material, Sec. V A [3]). This is the only organism for which a comprehensive map of neuronal connections within a brain has been reconstructed across development [5]. The dataset consists of eight fully reconstructed brains of the hermaphrodite *C. elegans*, obtained from different isogenic individuals at different developmental ages, including one at birth and two adults ($t \sim 45$ h after birth) (see Supplemental Material, Sec. V B [3]). We consider the unweighted and undirected networks of chemical synapses between sensory, inter, motor, and modulatory neurons (161–180 nodes and 617–1669 edges). This choice of representation is motivated by the statistical properties of the adult *C. elegans* connectome [9,10], along with the effort to devise a simplified growth model; a critical discussion can be found in Supplemental Material, Sec. V B [3].

The developmental principles that guide the *C. elegans* brain maturation are not entirely known. On the one hand, approximately 43% of the synaptic connections between neurons are not conserved among genetically identical individuals, suggesting a prominent role of stochasticity in the brain wiring [5,33]. Conversely, the diverse range of behaviors exhibited by adult *C. elegans* [35] demands functional selection. Our EE framework captures these two tendencies simultaneously. An overview of the approach is illustrated in Fig. 1. A microlevel interpretation of Eqs. (1) and (2) for the wiring dynamics of the individual neurons is extensively discussed in Supplemental Material, Sec. V C [3].

A preliminary step of our modeling approach is the characterization of the worm brain by a set of sufficient statistics $\boldsymbol{x}(G)$. Based on recent evidence [11,36], we consider a parsimonious representation in which

$$\boldsymbol{x}(G) = \begin{bmatrix} \sum_{k>0} w_{\tau_d}^{(k)} & x_d^{(k)}(G) \\ \sum_{k>0} w_{\tau_{\mathrm{esp}}}^{(k)} & x_{\mathrm{esp}}^{(k)}(G) \end{bmatrix}, \tag{3}$$

where $x_d^{(k)}$ and $x_{\mathrm{esp}}^{(k)}$ are the number of nodes with degree k and the number of connected dyads sharing exactly k partners, respectively. The coefficients are $w_\alpha^{(k)} = e^\alpha\{1-(1-e^{-\alpha})^k\}$, with $\alpha = \tau_d, \tau_{\mathrm{esp}} > 0$ decay parameters. In other words, these statistics are linear combinations of the degree and edgewise shared partner distributions.

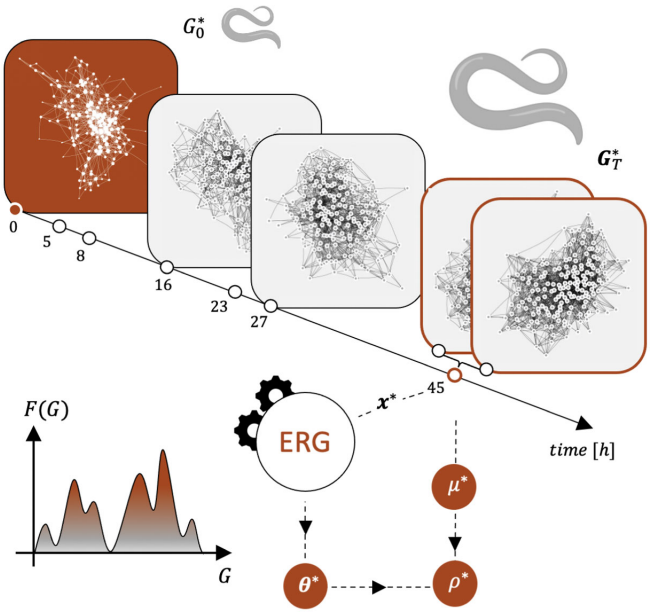

FIG. 1. EE dynamics for the *C. elegans* brain maturation. We consider the eight snapshots of the worm network of chemical synapses, at different developmental ages $t = 5, 8, 16, 23, 27$, and 45 h (two adults), from [5]—some are omitted for visual clarity. The birth configuration is fixed as the starting point of the dynamics. The two adult snapshots are used to infer (i) the topography of the functional landscape $F(G)$ (bottom left), encoded in the set $\boldsymbol{\theta}^*$—ERG inference starting from the empirical statistics $\boldsymbol{x}^* \equiv \boldsymbol{x}(\boldsymbol{G}_T^*)$; and (ii) the EE parameters, i.e., the exploration rate μ^* and the functional pressure ρ^*; see Supplemental Material, Sec. VI [3].

They yield a model that is both realistic and computationally tractable [12] (see Supplemental Material, Sec. IV [3]). More specifically, the first statistic is called geometrically weighted degree (gwd) and encodes the information, e.g., on the presence or absence of hub nodes in the graph, well documented in the case of *C. elegans* [5,11]. The second statistic is called geometrically weighted edgewise shared partner (gwesp) and is a proxy for a triadic-closure phenomenon in the graph; i.e., pairs of nodes that have links to one or more common neighbors have a higher chance of being connected to each other. The latter could, in turn, result from a tendency of the network to segregate into densely connected modules [5,11].

Given a choice of statistics as in Eq. (3), we can characterize any observed graph G^* within the inferential framework of exponential random graph (ERG) models [12,13] (see Supplemental Material, Sec. IV [3]). Accordingly, the ensemble $\mathcal{G}$ is endowed with a maximum entropy probability distribution

$$P_{\mathrm{ERGM}}(G|\boldsymbol{\theta}) = e^{-\mathcal{H}(G,\boldsymbol{\theta})} / \sum_{\tilde{G}\in\mathcal{G}} e^{-\mathcal{H}(\tilde{G},\boldsymbol{\theta})}, \tag{4}$$

where $\mathcal{H}(G,\boldsymbol{\theta}) = -\boldsymbol{\theta}\cdot\boldsymbol{x}(G)$ is the Hamiltonian. Given an observed graph G^*, the vector of parameters $\boldsymbol{\theta}^*$ can be inferred as approximate solution the maximum likelihood estimation problem $\boldsymbol{\theta}^* = \arg\max_{\boldsymbol{\theta}} \log P(G^*|\boldsymbol{\theta})$. The inferred parameters quantify the contribution of the associated statistics to the structure of the observed graph. For example, if the statistic x_α is non-negative, positive θ_α^* imply the existence of a bias toward graphs with higher-than-random values of x_α—given the rest of the model $\sum_{\beta\neq\alpha}\theta_\beta^* x_\beta$ [12] (see Supplemental Material, Sec. IV [3]).

We are now in the position to propose the following F metric for the *C. elegans* brain maturation:

$$F(G) = \boldsymbol{\theta}^*\cdot\boldsymbol{x}(G), \tag{5}$$

where $\boldsymbol{x}(G)$ are defined in Eq. (3). The parameters $\boldsymbol{\theta}^*$ are obtained from the ERG inference in the adult stage, so that the correct (functional) balance of model statistics can be achieved at the end of the developmental process. The topography of the *functional landscape* is genetically encoded and results from the combined effect of physical, genetic, and functional constraints.

In particular, we consider the average estimated parameters from the two adult worms $\boldsymbol{G}_T^* = (G_{T,1}^*, G_{T,2}^*)$ and obtain $\theta_{\mathrm{gwd}}^* = 0.44$ and $\theta_{\mathrm{gwesp}}^* = 0.58$ (see Supplemental Material, Sec. VI A [3]). EE dynamics based on Eq. (5) will favor both the emergence of hubs and of a triadic closure behavior, since, by virtue of the positive values of the linear parameters, higher values of the statistics in Eq. (3) will imply higher F values. This is in line with experimental observations that, during development, hub neurons at birth get more inputs and that the overall modularity of the *C. elegans* brain network increases [5].

We can now proceed to model the developmental dynamics by setting appropriate boundary conditions and the EE parameters of the dynamics: the exploration rate and the functional pressure. As the argument goes, μ and ρ are characteristic of the specific instance (*C. elegans*) of the biological process (brain wiring); they are genetically encoded and, therefore, result from the evolutionary history of the species.

We set the graph G_0^* corresponding to the network at birth as the starting point of the dynamics, $P(G = G_0^*, 0) = 1$. In fact, (i) as reported in [5], the brain morphology at birth serves as the structural foundation upon which the adult connectivity unfolds. Moreover, (ii) an implicit assumption of the EE graph dynamics is the *functional homogeneity*, i.e., that the same F metric holds true throughout the whole dynamics. This assumption is likely to be violated before hatching (birth), during the embryonic stage, where a different growth regime of the nervous system has been observed [37].

Throughout development, the removal of synaptic connections happens rarely [5]. Accordingly, we modify the mutation scheme described in Eq. (1) by restricting the removal of edges. By Occam's razor, we assume a constant exploration rate

$$\mu^* = \frac{1}{TL}\sum_{i<j}[\bar{a}_{ij}(\boldsymbol{G}_T^*) - a_{ij}(G_0^*)] = 1.43 \times 10^{-3}\ \mathrm{h}^{-1}, \quad (6)$$

where $T = 45$ h is the adult age, $L = N(N-1)/2$ is the number of dyads of the adult brain graphs ($N = 180$), $\sum_{i<j}\bar{a}_{ij}(\boldsymbol{G}_T^*)$ is the average number of edges between the two adult worms, and $\sum_{i<j}a_{ij}(G_0^*)$ is the number of edges at birth. At the end of the developmental dynamics, μ^* is assumed to drop to zero.

We are left with only one free parameter, i.e., the functional pressure $\rho = \varphi/\mu > 0$. Nonzero ρ describe the scenario in which new connections emerge primarily in locations where they result in an enhanced system function. Its value must be biologically regulated to ensure the development of adequately specialized functional circuits prior to reaching the adult stage. Therefore, we use the corresponding degree of freedom to inform the EE graph dynamics about the age of the adulthood. In particular, we set $\rho^* = \min_\rho \delta_T^{\mathrm{mah}}$, where the quantity to be minimized is the Mahalanobis distance [14], at time T, between the two-dimensional ensemble distribution of the graph statistics and the average experimental values (see Supplemental Material, Sec. VI B [3]).

In Fig. 2(a), we show that δ_T^{mah} is a convex function of the functional pressure ρ. Both insufficient and excessive ρ lead to the ensemble distribution diverging from the experimental values. The minimization procedure yields $\rho^* = 9.017 \times 10^2$ ($R^2 = 0.98$).

Notably, in estimating the dynamical parameters we have relied solely on the *C. elegans* brain graphs at birth and in the adult stage. We can ask if and how the estimation would change when considering the whole available data, which include the developmental time points at 5, 8, 16, 23, 27, and 45 h after birth. A linear fit of the growth of the number of edges based on the whole time series yields $\mu^{**} = (1.39 \pm 0.08) \times 10^{-3}\ \mathrm{h}^{-1}$. This estimation is compatible with the value μ^* in Eq. (6) [Fig. 2(b)]. As for the functional pressure, we can define an equivalent minimization problem where the Mahalanobis distance is summed over all experimental time points, yielding a value ρ^{**} that is statistically consistent with ρ^* [see Fig. 2(a) and Supplemental Material, Sec. VI B [3]].

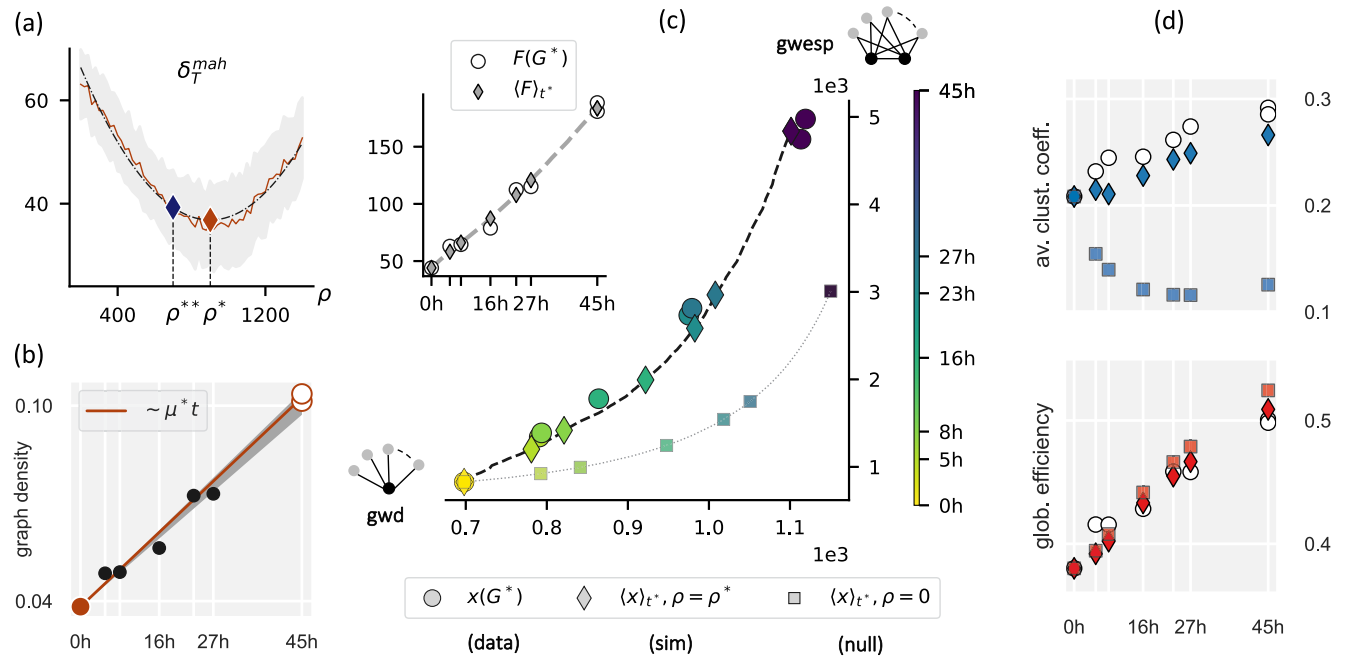

FIG. 2. Tracking down the *C. elegans* brain maturation. (a) We run 100 simulations $\forall\ \rho \in \{200 + 20i, 0 \le i \le 60\}$. For each ρ, we compute the mean and standard deviation of δ_T^{mah} (red line and shaded area, respectively). We fit the data with a quadratic curve (dash-dotted line) and take the abscissa ρ^* of its minimum (red diamond) as an estimation of the functional pressure. On the same curve, we show the value (blue diamond) corresponding to the abscissa ρ^{**} we get by minimizing the sum of the Mahalanobis distances over all experimental time points (see Supplemental Material, Sec. VI B [3]). The two overlap within the error bars. (b) The exploration rate is calculated by using the first and last time points (average). The shaded area corresponds to the estimation by a linear fit over the whole time series. (c) One simulation run with μ^*, ρ^*. Main: the trajectory in the space of statistics (gwd and gwesp). Experimental data (circles) are closely tracked by our simulations (dashed line, diamonds highlighting the *observed* time points $\boldsymbol{t}^*$). The trajectory of a null model with $\rho = 0$ is also shown (dotted line, squares). Inset: the simulated and experimental time course of F in time. (d) Feature generalization. The temporal trajectory of the average clustering coefficient and global efficiency, markers as described in (c). See also Supplemental Material, Sec. VI C [3].

This hints that (i) given the model in Eq. (5), the assumption of functional homogeneity for the worm brain wiring dynamics holds true and (ii) the EE graph dynamics, informed about birth and adulthood, capture the entire developmental trajectory.

To further investigate this result, we can fix μ^*, ρ^* and look at individual simulations of the brain growth, as in Fig. 2(c). For comparison, we also plot the results of a null model where $\rho = 0$, i.e., a random graph growth with exploration rate μ^*. As could be expected, the adult stage is correctly reached in terms of the model statistics in Eq. (3) and, by consequence, of the F metric. Notably, however, our simulations approximate *en passant* the other observed developmental ages, which we have used nowhere in inferring the parameters. This opens up the possibility of using our framework to reconstruct also those stages of brain maturation for which no data are available.

The model described so far is a simple, low-dimensional model of the underlying biological dynamics. Almost by construction, a choice as simple as Eq. (3) is unlikely to capture the finer-scale topological details of the observed graphs. Analogously, an exploration dynamics as simple as Eq. (6) cannot capture transient dynamic patterns. Yet, we can meaningfully ask to what extent the EE graph dynamics based on the features in Eq. (3) reproduces other network properties not included in the model formulation (see Supplemental Material, Sec. VI C [3]). In Fig. 2(d), we show that our model retrieves the propensity of the *C. elegans* brain networks to exhibit relatively high efficiency (like random graphs) and clustering (unlike random graphs) [15].

Discussion.—In summary, we have presented a parsimonious, interpretable framework for the dynamics of networked biological systems. It is built upon the dynamical principle of the exploration-exploitation paradigm, which is general. It serves as theoretical scaffolding for formulating specific dynamical models, which must be tailored to the biological system. We have used it here to model the growth of the *C. elegans* connectome, from birth to adulthood. Notably, our results suggest that the knowledge of the birth and adult age is sufficient for the EE graph dynamics to describe the whole developmental trajectory. We speculate that the same may be true for the connectomes of other living systems [38–40], for which no such data as the developmental trajectory are available to date. This hypothesis is poised for experimental validation in the near future.

Our model should be regarded as a first step toward a more detailed understanding of the brain maturation. To this end, the framework here presented supports straightforward extensions to more complex exploration schemes, accounting for nonuniform synapse addition, directed flow of synaptic information, neuron-specific information, homophily effects, and physical or functional constraints [5,11]. A detailed discussion of the possible model extensions can be found in Supplemental Material, Sec. VII A [3]. Beyond structural connectivity, it would be interesting to study under the same lens the *C. elegans* brain functional connectivity, recently mapped for the adult stage [41], where there exists a closer correlation between the notion of biological function and the topology of the graph.

Zooming out, our framework can be broadly used to study the dynamics of complex systems arising from the interplay between (i) the variability fueled by a stochastic search of the configuration space and (ii) the state-dependent optimization of an objective function—we propose three examples in Supplemental Material, Sec. VII B [3]. Importantly, as showcased here, this can be done by introducing only a very limited number of interpretable parameters [3,42].

We thank E. Aurell, E. Mauri, D. Battaglia, and M. Josserand for the many useful discussions. F. D. V. F. acknowledges support from the European Research Council (ERC), Grant Agreement No. 864729.

*Corresponding author: fabrizio.de-vico-fallani@inria.fr

[1] W. Bialek, *Biophysics: Searching for Principles* (Princeton University Press, Princeton, NJ, 2012).
[2] J. F. Crow and M. Kimura, *An Introduction to Population Genetics Theory* (Scientific Publishers, Princeton, NJ, 2017).
[3] See Supplemental Material at http://link.aps.org/supplemental/10.1103/PhysRevLett.132.098402 for additional discussion, which includes Refs. [4–32].
[4] V. Dichio, The exploration-exploitation paradigm: A biophysical approach, Ph.D. thesis, Sorbonne Université, 2023, https://arxiv.org/abs/2312.14850.
[5] D. Witvliet, B. Mulcahy, J. K. Mitchell, Y. Meirovitch, D. R. Berger, Y. Wu, Y. Liu, W. X. Koh, R. Parvathala, D. Holmyard *et al.*, Nature (London) **596**, 257 (2021).
[6] V. Dichio, H. Zeng, and E. Aurell, Rep. Prog. Phys. **86**, 052601 (2023).
[7] D. Goldberg, *Genetic Algorithms in Search, Optimization, and Machine Learning* (Addison-Wesley, Reading, MA, 1989).
[8] J. G. White, E. Southgate, J. N. Thomson, S. Brenner *et al.*, Phil. Trans. R. Soc. B **314**, 1 (1986).
[9] L. R. Varshney, B. L. Chen, E. Paniagua, D. H. Hall, and D. B. Chklovskii, PLoS Comput. Biol. **7**, e1001066 (2011).
[10] S. J. Cook, T. A. Jarrell, C. A. Brittin, Y. Wang, A. E. Bloniarz, M. A. Yakovlev, K. C. Nguyen, L. T.-H. Tang, E. A. Bayer, J. S. Duerr *et al.*, Nature (London) **571**, 63 (2019).
[11] A. Pathak, N. Chatterjee, and S. Sinha, PLoS Comput. Biol. **16**, e1007602 (2020).
[12] V. Dichio and F. De Vico Fallani, Rep. Prog. Phys. **86**, 102601 (2023).
[13] G. Cimini, T. Squartini, F. Saracco, D. Garlaschelli, A. Gabrielli, and G. Caldarelli, Nat. Rev. Phys. **1**, 58 (2019).

[14] P. C. Mahalanobis, Proc. Natl. Inst. Sci. (Calcutta) **2**, 49 (1936), https://www.jstor.org/stable/48723335.
[15] V. Latora, V. Nicosia, and G. Russo, *Complex Networks: Principles, Methods and Applications* (Cambridge University Press, Cambridge, England, 2017).
[16] M. B. Hamilton, *Population Genetics* (John Wiley & Sons, New York, 2021).
[17] S. Manrubia, J. A. Cuesta, J. Aguirre, S. E. Ahnert, L. Altenberg, A. V. Cano, P. Catalán, R. Diaz-Uriarte, S. F. Elena, J. A. García-Martín *et al.*, Phys. Life Rev. **38**, 55 (2021).
[18] F. Zanini and R. A. Neher, Bioinformatics **28**, 3332 (2012).
[19] E. Mauri, S. Cocco, and R. Monasson, Europhys. Lett. **132**, 56001 (2021).
[20] R. Albert and A.-L. Barabási, Rev. Mod. Phys. **74**, 47 (2002).
[21] E. T. Jaynes, Phys. Rev. **106**, 620 (1957).
[22] C. J. Geyer, Stat. Sci. **7**, 473 (1992), https://hdl.handle.net/11299/58440.
[23] P. N. Krivitsky, M. S. Handcock, D. R. Hunter, C. T. Butts, C. Klumb, S. M. Goodreau, and M. Morris, J. Stat. Software **24**, 1 (2008).
[24] M. Schweinberger, P. N. Krivitsky, C. T. Butts, and J. R. Stewart, Stat. Sci. **35**, 627 (2020).
[25] D. R. Hunter, Soc. Networks **29**, 216 (2007).
[26] B. Bentley, R. Branicky, C. L. Barnes, Y. L. Chew, E. Yemini, E. T. Bullmore, P. E. Vértes, and W. R. Schafer, PLoS Comput. Biol. **12**, e1005283 (2016).
[27] M. Skuhersky, T. Wu, E. Yemini, A. Nejatbakhsh, E. Boyden, and M. Tegmark, BMC Bioinf. **23**, 1 (2022).
[28] G. Rapti, J. Neurogen. **34**, 259 (2020).
[29] D. A. Colón-Ramos, Curr. Top. Dev. Biol. **87**, 53 (2009).
[30] A. Kessy, A. Lewin, and K. Strimmer, Am. Stat. **72**, 309 (2018).
[31] V. Dichio, EE-graph-dyn, GitHub folder (2023), https://github.com/dichio/EE-graph-dyn.
[32] R. A. Neher and B. I. Shraiman, Rev. Mod. Phys. **83**, 1283 (2011).
[33] B. A. Hassan and P. R. Hiesinger, Cell **163**, 285 (2015).
[34] N. Goldenfeld and C. Woese, Annu. Rev. Condens. Matter Phys. **2**, 375 (2011).
[35] M. de Bono and A. Villu Maricq, Annu. Rev. Neurosci. **28**, 451 (2005).
[36] A. Azulay, E. Itskovits, and A. Zaslaver, PLoS Comput. Biol. **12**, e1005021 (2016).
[37] V. Nicosia, P. E. Vértes, W. R. Schafer, V. Latora, and E. T. Bullmore, Proc. Natl. Acad. Sci. U.S.A. **110**, 7880 (2013).
[38] D. G. C. Hildebrand, M. Cicconet, R. M. Torres, W. Choi, T. M. Quan, J. Moon, A. W. Wetzel, A. Scott Champion, B. J. Graham, O. Randlett *et al.*, Nature (London) **545**, 345 (2017).
[39] L. K. Scheffer, C. S. Xu, M. Januszewski, Z. Lu, S.-y. Takemura, K. J. Hayworth, G. B. Huang, K. Shinomiya, J. Maitlin-Shepard, S. Berg *et al.*, eLife **9**, e57443 (2020).
[40] L. F. Abbott, D. D. Bock, E. M. Callaway, W. Denk, C. Dulac, A. L. Fairhall, I. Fiete, K. M. Harris, M. Helmstaedter, V. Jain *et al.*, Cell **182**, 1372 (2020).
[41] F. Randi, A. K. Sharma, S. Dvali, and A. M. Leifer, Nature (London) **623**, 406 (2023).
[42] F. Dyson, Nature (London) **427**, 297 (2004).